JOURNAL OF SPACECRAFT AND ROCKETS
Vol. 34, No. 6, November–December 1997

Experimental Rarefied Heat Transfer at Hypersonic Conditions over 70-Degree Blunted Cone

J. Allègre,* D. Bisch,† and J. C. Lengrand‡
Centre National de la Recherche Scientifique, 92190 Meudon, France

Surface heat transfer rates have been measured over a 70-deg spherically blunted cone chosen as a test case model to provide both experimental and computational databases. Under rarefied and hypersonic conditions, heating rate distributions are measured along the model and presented at angles of attack varying from 0 to 30 deg. Experiments have been conducted in the SR3 facility at a freestream Mach number close to 20. Three flow rarefactions have been considered, which correspond to Reynolds numbers of 1420, 4175, and 36,265. Reynolds numbers are calculated using freestream conditions and the model base diameter. In parallel to the experimental work, flow calculations were executed by an international group of researchers for identical test conditions. Comparisons between experimental and computational heating rates are also presented.

Nomenclature

c = specific heat, kJ/kg/K
d = base diameter, 50 mm
e = wall thickness, mm
l = thermocouple signal, μV
Ma = nominal freestream Mach number
p_0 = stagnation pressure, bar
q = heating rate, kW/m^2
R_C = corner radius, mm
Re_d = Reynolds number calculated on the base diameter
R_n = nose radius, mm
S = abscissa along the model, measured from the stagnation point, mm
T = temperature, K
T_0 = stagnation temperature, K
T_W = surface temperature, K
t = time, s
V = freestream velocity, m/s
$\bar{V}$ = rarefaction parameter, $Ma/(Re_d)^{0.5}$
α = angle of attack, deg
ρ = model-wall density, kg/m^3
ρ_∞ = freestream density, kg/m^3

Introduction

As part of AGARD, the Fluid Dynamics Panel and its Working Group 18 have chosen the 70-deg spherically blunted cone as the test case model. In the rarefied and hypersonic domain, a number of experiments have been performed over the blunted cone to get quantitative aerothermodynamic results with the objective of code validation by comparisons between experimental and computational data. Two companion papers were focused on the presentation of experimental density flowfields and on aerodynamic forces applied to the model.[1,2] This paper provides experimental heating rate data for the forebody, the base section, and the rear sting of the blunted cone. Some experimental results have been presented to the Fourth European High Velocity Database Workshop[3]; the present paper exhibits complete sets of experimental heat transfer data. Test conditions are characterized by a freestream Mach number close to 20 and by Reynolds numbers ranging from 1420 to 36,265. Reynolds numbers are calculated using freestream conditions and the cone base diameter. Heating rates are measured for three rarefaction levels and for cone angles of attack between 0 and 30 deg.

Blunted Cone Model and Measurement Technique

The spherically blunted cone used for heat flux measurements is composed of thin-wall elements (Fig. 1). It is made of ARMCO steel of well-known thermal characteristics. The cone base diameter is 50 mm. The rear sting diameter is 12.5 mm with a useful length of 75 mm. The sting extremity is connected to a movable transverse support used to inject the model through the test section. The transverse support is actuated by means of a mechanism with a pneumatic jack located outside the test section. The model is instrumented with Ch/Al thermocouples embedded through the wall thickness. Heat transfer measurements are performed at nine locations distributed along the forebody, along the base, and along the cylindrical sting. Thermocouple references and locations are specified in Fig. 2.

The thin-wall technique is one of the most accurate methods used for measuring heat fluxes. The measurement procedure consists of starting the wind tunnel without the model, and as soon as the flow conditions are constant, the thin-wall model is rapidly injected through the test section. The surface temperature is locally measured using thermocouples embedded in the wall. Knowing locally the thickness e of the model wall and the thermal capacity of the material ρc, the measured derivative of the wall temperature T_W is directly related to the heat flux value q, using the formula $q = \rho ce(\mathrm{d}T_W/\mathrm{d}t)$. For the present experiments, Ch/Al thermocouple wires, 0.2 mm in diameter, are embedded in the thin wall, which is 0.4 mm thick in mean value. The exact wall thickness has been measured at each point of measurement to calculate heating rate values. For the ARMCO steel, density and specific heat values are $\rho = 7.86 \times 10^3$ kg/m^3 and $c = 0.449$ kJ/kg/K, respectively. Prior to heat flux measurements, the cone model is located outside the test section at room temperature. At the time of the measurement, just following the model injection through the test section, the wall temperature of the model remains close to 300 K. To minimize conduction effects through the wall, the temperature derivative is measured within fractions of a second following the model injection, limiting to a few degrees only the wall-temperature rise during the measurement.

Test Facility and Flow Conditions

The SR3 wind tunnel is equipped with pumping systems working in continuous operation. According to the required flow conditions, two distinct pumping groups are used. At the lowest flow densities (first and second set of flow conditions), the exhaust system is composed of rotary piston vacuum pumps, Roots pumps, and oil diffusion booster pumps, withstanding volume flow rates of air or nitrogen of about 40 m^3/s under working pressures up to 10^{-4} atm.

Received Jan. 9, 1997; revision received July 3, 1997; accepted for publication July 11, 1997.

*Research Engineer, Department of Hypersonics and Rarefied Flow, 4 ter route des Gardes.
†Research Assistant, Department of Hypersonics and Rarefied Flow, 4 ter route des Gardes.
‡Head, Laboratoire d'Aérothermique, 4 ter route des Gardes. Member AIAA.

At higher flow densities (third set of flow conditions), the exhaust system includes rotary sliding vane pumps and Roots pumps.

Heating rate measurements are performed at hypersonic and rarefied flow conditions for three rarefaction levels. The nominal operating conditions are indicated in Table 1. Nitrogen flows are issued from three different nozzles supplied with an electrical graphite heater. Divergent sections of the nozzles are conical and continued by cylindrical extensions providing the junction between the conical parts and the test section. Reynolds numbers Re_d and rarefaction parameters [$\bar{V} = Ma/(Re_d)^{0.5}$] have been calculated assuming, as a reference, the 5-cm base diameter. The Sutherland viscosity law is applied for gas temperatures down to 100 K, and then a linear viscosity law is used at lower gas temperatures between 0 and 100 K. Mach numbers indicated in Table 1 are the freestream Mach numbers at the nose location of the blunted cone, where flow parameters are assumed to take their nominal values.

Results and Discussion

Tabulated values of heating rates are presented in Tables 2–4 for the three flow conditions. In each table one will find successively the thermocouple references, the corresponding nondimensional distances S/R_n, the angles of attack of the model, and the measured heating rates. The tables are composed of three parts covering the forebody region (thermocouples 1–4), the base region (thermocouples 5 and 6), and the rear sting region (thermocouples 7–9). Heating rates are given for the angles of attack of 0, 10, 20, and 30 deg.

The overall heating rate distributions along the blunted cone have been plotted in Figs. 3–9 as a function of the nondimensional distance S/R_n measured along the surface from the forebody stagnation point. At an angle of attack of 20 deg and for the three flow conditions, heating rate distributions are successively presented in Figs. 3–5. Maximum over the forebody region, heating rates range from about 7 to 46 kW/m^2, depending on the flow rarefactions. On the base surface, the measured heating rates are extremely low. They are found to be less than 0.02 kW/m^2 for the most rarefied flow and of the order of 0.6 kW/m^2 for the highest flow density. Along the rear sting, the highly expanded flow still leads to low values of heating

Table 1 SR3 wind tunnel experimental test conditions

Flow conditions	Gas	Ma	T_0, K	p_0, bars	Re_d	$\bar{V}$
1	N_2	20.2	1,100	3.5	1,420	0.53
2	N_2	20	1,100	10	4,175	0.31
3	N_2	20.5	1,300	120	36,265	0.11

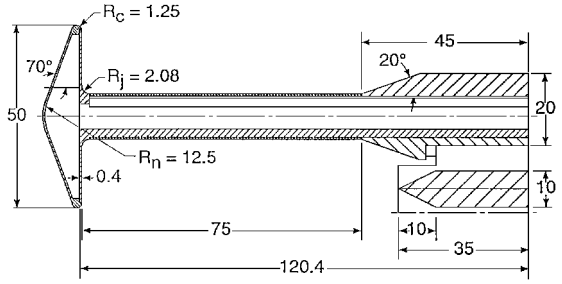

Fig. 1 Thin-wall test model for heat transfer measurements. All dimensions are in millimeters.

Table 2 Heating rates (test conditions 1: Ma = 20.2, Re_d = 1420)

		q, kW/m^2			
Thermocouple	S/R_n	$\alpha = 0$ deg	$\alpha = 10$ deg	$\alpha = 20$ deg	$\alpha = 30$ deg
1	0	10.23	9.89	7.59	6.60
2	0.52	8.39	8.07	6.78	5.81
3	1.04	6.33	6.93	6.93	5.72
4	1.56	5.12	6.63	7.53	7.23
5	2.68	<0.02	<0.02	<0.02	<0.02
6	3.32	<0.02	<0.02	<0.02	<0.02
7	5.06	0.13	0.20	0.33	0.59
8	6.50	0.33	0.46	1.22	2.04
9	7.94	0.43	0.82	1.58	2.70

Table 3 Heating rates (test conditions 2: Ma = 20, Re_d = 4175)

		q, kW/m^2			
Thermocouple	S/R_n	$\alpha = 0$ deg	$\alpha = 10$ deg	$\alpha = 20$ deg	$\alpha = 30$ deg
1	0	17.16	17.82	15.84	14.19
2	0.52	13.56	16.46	15.17	14.85
3	1.04	10.24	14.16	12.95	14.46
4	1.56	9.64	12.05	13.56	15.06
5	2.68	<0.04	<0.04	<0.04	<0.04
6	3.32	<0.04	<0.04	<0.04	<0.04
7	5.06	0.43	1.06	1.95	3.79
8	6.50	0.99	2.18	3.00	5.94
9	7.94	1.75	2.38	3.83	8.58

Table 4 Heating rates (test conditions 3: Ma = 20.5, Re_d = 36,265)

		q, kW/m^2			
Thermocouple	S/R_n	$\alpha = 0$ deg	$\alpha = 10$ deg	$\alpha = 20$ deg	$\alpha = 30$ deg
1	0	67.97	59.39	46.19	44.87
2	0.52	50.35	49.71	43.57	45.19
3	1.04	34.94	44.59	42.17	44.58
4	1.56	27.71	42.17	42.78	46.39
5	2.68	0.59	0.53	0.59	0.73
6	3.32	0.46	0.46	0.66	0.89
7	5.06	1.65	2.77	7.59	14.19
8	6.50	3.10	7.92	14.19	19.80
9	7.94	3.79	11.22	14.19	18.81

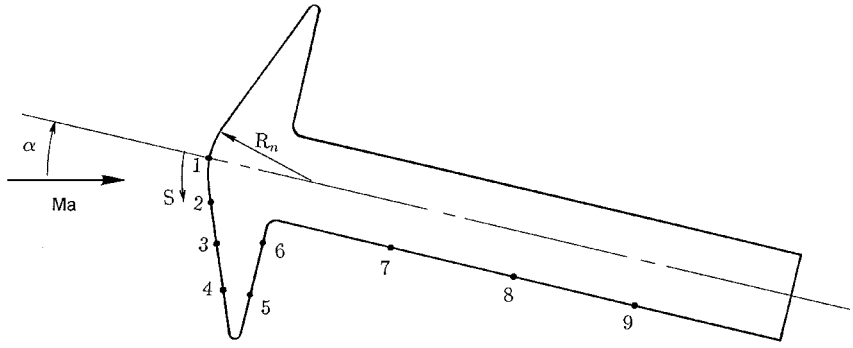

Thermocouples	1	2	3	4	5	6	7	8	9
Location S/Rn (Rn = 12.5 mm)	0.00	0.52	1.04	1.56	2.68	3.32	5.06	6.50	7.94

Fig. 2 Thermocouple locations along the test model.

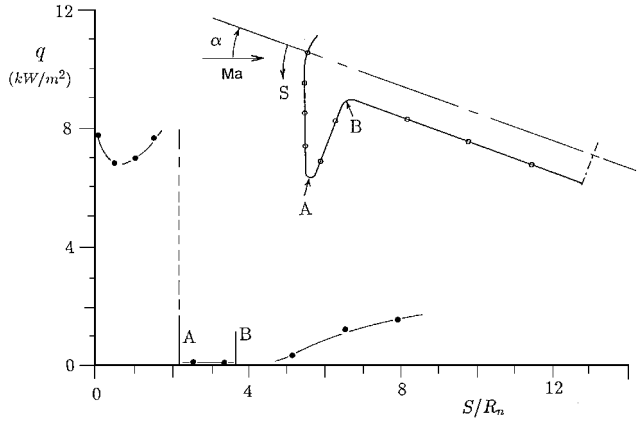

Fig. 3 Heating rate distribution: $Ma = 20.2$, $Re_d = 1420$, and $\alpha = 20$ deg (first set of flow conditions).

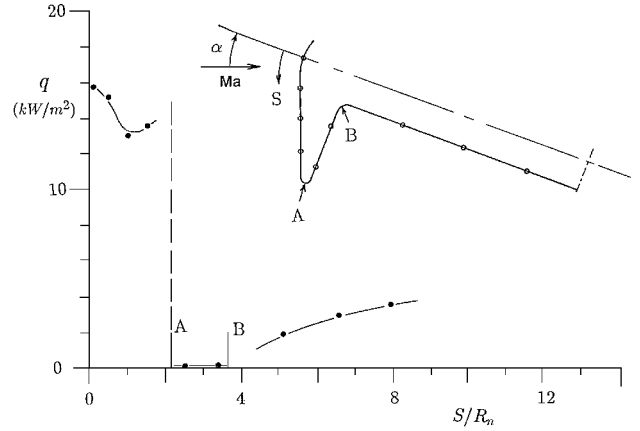

Fig. 4 Heating rate distribution: $Ma = 20$, $Re_d = 4175$, and $\alpha = 20$ deg (second set of flow conditions).

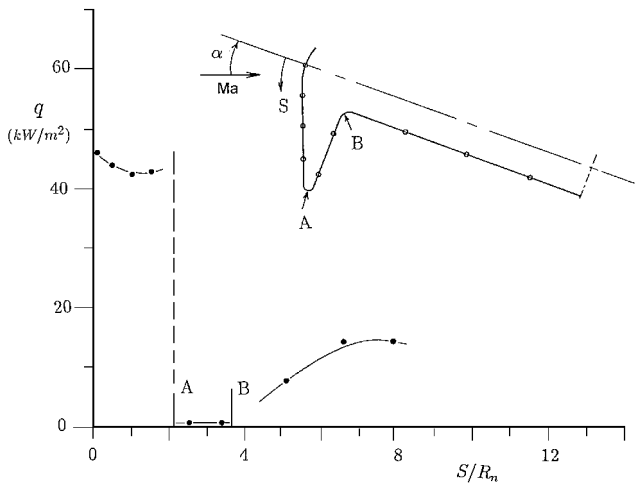

Fig. 5 Heating rate distribution: $Ma = 20.5$, $Re_d = 36{,}265$, and $\alpha = 20$ deg (third set of flow conditions).

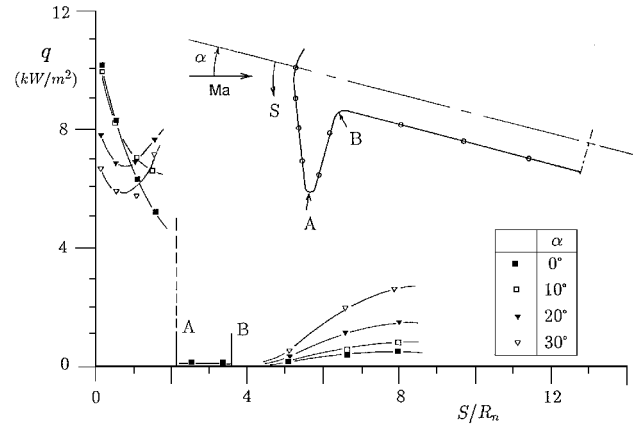

Fig. 6 Heating rate distributions: $Ma = 20.2$, $Re_d = 1420$, and $0 \leq \alpha \leq 30$ deg (first set of flow conditions).

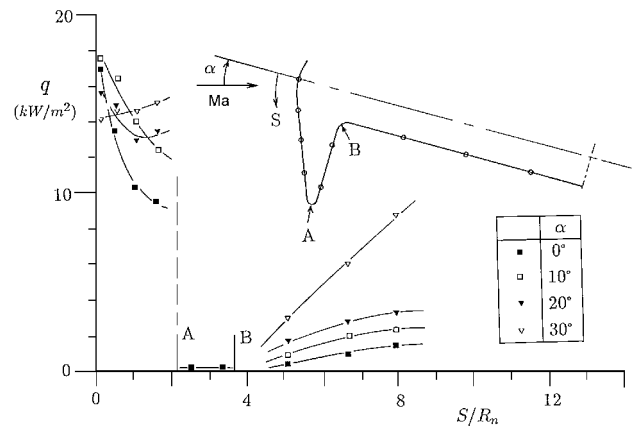

Fig. 7 Heating rate distributions: $Ma = 20$, $Re_d = 4175$, and $0 \leq \alpha \leq 30$ deg (second set of flow conditions).

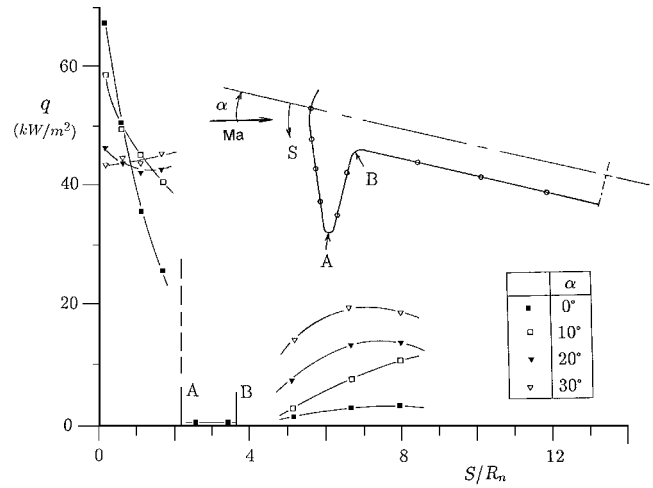

Fig. 8 Heating rate distributions: $Ma = 20.5$, $Re_d = 36{,}265$, and $0 \leq \alpha \leq 30$ deg (third set of flow conditions).

rates; however, values are slightly increased when one moves farther downstream.

Considering different angles of attack of the blunted cone from 0 up to 30 deg, heating rate distributions are indicated in Figs. 6–8 for the three rarefaction levels. When increasing the angle of attack, heating rate distributions become more uniform along the forebody region and, also, heating rate values increase quite markedly along the rear sting surface. Last, at 0-deg angle of attack, heating rate distributions are plotted in Fig. 9 considering the three rarefaction levels of the flow. Along the forebody region, the heating rate is maximum at the stagnation point and then decreases when moving aft of the stagnation point. Maximum heating rates vary from about 10 to 68 kW/m^2 according to the flow rarefaction.

As part of AGARD, the Fluid Dynamic Panel and its Working Group 18 assumed the coordination of blunt-body investigations for hypersonic conditions. Studies have been conducted both for high-enthalpy tests obtained with impulse facilities[4,5] and for rarefied tests performed in rarefied low-enthalpy facilities.[1,6] In parallel to the present experimental work, a number of calculations using a direct simulation Monte Carlo solution were executed by an international group of researchers. An extensive number of computations have been made over the blunted cone for SR3 test conditions

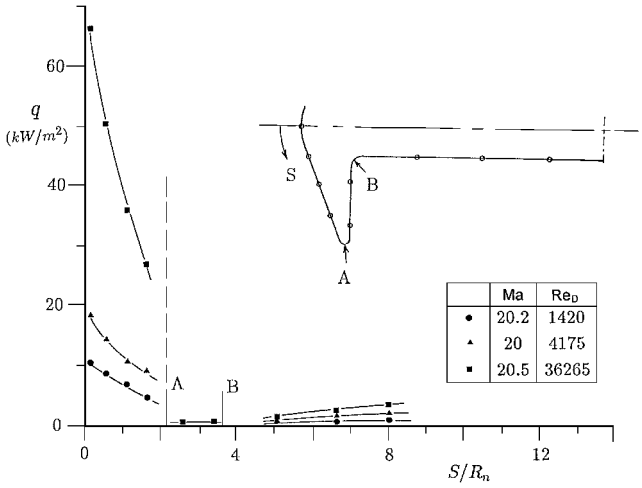

Fig. 9 Heating rate distributions: $\alpha = 0$ deg and $1420 \leq Re_d \leq 36{,}265$.

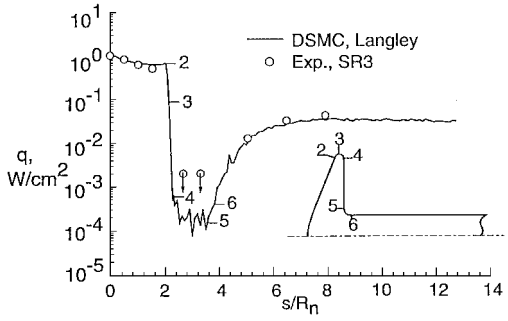

Fig. 10 Experimental and calculated heating rates (SR3 first set of flow conditions, NASA Langley Research Center computations).

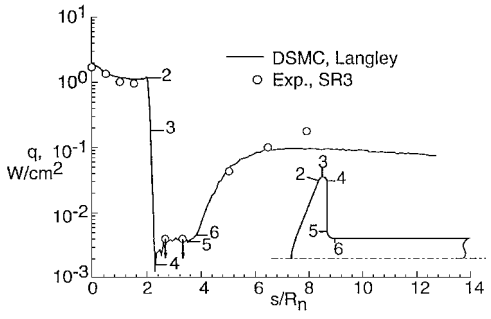

Fig. 11 Experimental and calculated heating rates (SR3 second set of flow conditions, NASA Langley Research Center computations).

because it was one of the test cases at the Fourth European High-Velocity Database Workshop. Some results were included at the workshop and were indicative of good agreements achieved between computation and experiment.[3,7]

Comparisons between computed heating rates and experimental heating rates have already been presented.[7–9] To illustrate some of these comparisons, heating rates calculated by Moss et al.[8] and heating rates measured in the SR3 wind tunnel are shown in Figs. 10–12 for the three sets of experimental conditions.

Accuracy of Heating Rate Measurements

Data uncertainty in heating rate measurements may result from different causes: uncertainty due to the determination of the model-wall heat capacity, uncertainty in the measurement of the wall temperature derivative, and uncertainty due to possible heat conduction effects through the thin wall at the time of the measurement. The ARMCO steel used for manufacturing the model has a well-known heat capacity, and the wall thickness is measured at each thermocouple location with an estimated uncertainty of $\pm 2\%$.

The determination of the wall-temperature derivative contributes, in a larger part, to the measurement uncertainty. Its level depends on

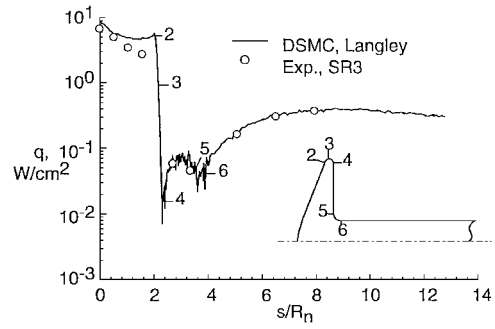

Fig. 12 Experimental and calculated heating rates (SR3 third set of flow conditions, NASA Langley Research Center computations).

the signal amplitude and, in most cases, the uncertainty is less than $\pm 5\%$. Concerning Ch/Al thermocouples, they deliver an output signal of about 41 μV/K at room temperature, the output voltage being slightly decreased for lower temperatures (40 μV/K at 280 K) and slightly increased for higher temperatures (41.5 μV/K at 320 K). All measurements are made during a fraction of a second following the model injection through the test section and, consequently, the wall-temperature variation remains within the range 290–310 K. This justifies the use of 41 μV/K when calculating the wall temperature from the measured thermocouple signal.

Regarding conduction effects, they are negligible for most of the present conditions. That is the case for the first set and the second set of flow conditions ($Re_d = 1420$ and 4175) and all investigated surfaces (forebody, base, and rear sting). Measured wall-temperature variations are less than 10 K/s at the time of the measurement and, consequently, temperature differences through the wall do not exceed a couple of Kelvin during the first fractions of a second corresponding to the heating rate determination. For the third set of flow conditions ($Re_d = 36{,}265$), also small variations of wall temperatures are recorded in the base and rear sting regions and negligible conduction effects are expected. However, on the forebody, wall-temperature variations as high as 37 K/s are recorded, leading to larger temperature differences along the thin wall with possible local conduction effects. Heat conduction is difficult to quantify; it depends on temperature gradients along the thin wall and is certainly maximum in the peripheral region linking the forebody to the base region. Consequently, for the third set of flow conditions, heat measurements performed with thermocouple 4 may lead locally to underestimated values of heating rates.

For the reasons mentioned before, at practically all test conditions (except for the thermocouple 4 at the highest flow density), heating rates have been measured with a global uncertainty less than 10%.

Concluding Remarks

Experimental heating-rate distributions are presented over a 70-deg blunted cone located at rarefied and hypersonic flow conditions. The flow is characterized by a freestream Mach number close to 20 and three levels of gas rarefaction. Freestream Reynolds numbers, calculated on the cone base diameter, range from 1420 to 36,265. Local heating rates, measured by means of the thin-wall technique, are recorded for various angles of attack of the blunted cone between 0 and 30 deg. Heating rate distributions are presented along the forebody surface, the base surface, and the rear-sting surface. The present investigation provides quantitative information for code validation by making comparisons between experimental and computational data.

Acknowledgments

This work was supported by the European Space Agency (ESA-ESTEC) under Contracts 132622 and 133790.

References

[1] Allègre, J., Bisch, D., and Lengrand, J. C., "Experimental Rarefied Density Flowfields at Hypersonic Conditions over 70-Degree Blunted Cone," *Journal of Spacecraft and Rockets*, Vol. 34, No. 6, 1997, pp. 714–718.

[2]Allègre, J., Bisch, D., and Lengrand, J. C., "Experimental Rarefied Aerodynamic Forces at Hypersonic Conditions over 70-Degree Blunted Cone," *Journal of Spacecraft and Rockets*, Vol. 34, No. 6, 1997, pp. 719–723.

[3]Coron, F., and Harvey, J. K., "Synopsis for Test Case 6—Rarefied 70 Degree Spherically Blunted Cone Flow," Fourth European High-Velocity Database Workshop, ESTEC, Noordwijk, The Netherlands, Nov. 1994.

[4]Gochberg, L. A., Allen, G. A., Gallis, M. A., and Deiwert, G. S., "Comparison of Computations and Experiments for Nonequilibrium Flow Expansions Around a Blunted Cone," AIAA Paper 96-0231, Jan. 1996.

[5]Holden, M., Harvey, J., Boyd, I., George, J., and Horvath, T., "Experimental and Computational Studies of the Flow over a Sting Mounted Planetary Probe Configuration," AIAA Paper 97-0768, Jan. 1997.

[6]Danckert, A., and Legge, H., "Wake Structure of a 70 Degree Blunted Cone, DSMC Results and Patterson Probe Measurements," AIAA Paper 95-2141, June 1995.

[7]Moss, J. N., Price, J. M., and Dogra, V. K., "DSMC Calculations for a Spherically Blunted Cone," Fourth European High-Velocity Database Workshop, ESTEC, Noordwijk, The Netherlands, Nov. 1994.

[8]Moss, J. N., Price, J. M., Dogra, V. K., and Hash, D. B., "Comparison of DSMC and Experimental Results for Hypersonic External Flows," AIAA Paper 95-2028, June 1995.

[9]Moss, J. N., and Price, J. M., "Review of Blunt Body Wake Flows at Hypersonic Low Density Conditions," AIAA Paper 96-1803, June 1996.

I. D. Boyd
Associate Editor